Scientific Research

Plastic Deformation Mechanisms of Base Material and Friction Stir Welded AZ31B-H24 Magnesium Alloy

Michael Regev[1], Stefano Spigarelli[2]

[1]Department of Mechanical Engineering, ORT Braude College, Karmiel, Israel; [2]Dipartimento di Meccanica, Università Politecnicadelle Marche, Ancona, Italy.
Email: michaelr@braude.ac.il

ABSTRACT

The friction stir welding process (FSW) was developed in the United Kingdom in the early 1990s. During FSW, the frictional heat that is generated is effectively utilized to facilitate material consolidation and eventual joining with the aid of axial pressure. The process is, therefore, a non-fusion welding process. FSW was applied in the current study in order to weld AZ31B-H24 alloy plates. Each of the different zones of the welded joint underwent optical metallographic characterization: the parent material, the Heat Affected Zone (HAZ), the Thermo-Mechanically Affected Zone (TMAZ), and the weld nugget. Optical metallography revealed deformation twinning at the TMAZ, grain refinement at the HAZ and evidence of heavy plastic deformation at the nugget. Creep tests at 100°C, 200°C and 300°C were conducted both on the parent material and on the friction stir welded specimens. Two different creep regimes seem to exist, a high stress regime in which creep is controlled by dislocation climb, and a low stress regime in which Grain-Boundary Sliding (GBS) becomes the dominant mechanism. Transmission electron microscopy of welded and non-welded specimens that underwent creep at 100°C revealed the existence of dislocation segments that do not lie on the basal planes. It is therefore assumed that other slip systems are active, in addition to the $\langle 11\bar{2}0 \rangle \{0001\}$ basal slip systems known to be the only ones active in pure magnesium up to about 180°C. The proposed deformation mechanism involves dislocation gliding on basal and non-basal planes assisted by twinning and GBS.

Keywords: Friction Stir Welding; Magnesium Alloys; AZ31; Creep; Dislocations

1. Introduction

The deformation mechanisms of pure magnesium are well known and are discussed in many publications, such as [1-3]. Researchers in the field agree that plastic deformation occurs on basal slip systems at room temperature, while at temperatures higher than 225°C, prismatic and pyramidal systems become active as well. This in turn dictates relatively low elongation-to-fracture of pure magnesium up to about 225°C. Since AZ31 (Al 3%, Zn 1%), on the contrary, exhibits large elongation-to-fracture (around 15%) even at room temperature [4], different operative deformation mechanisms can be expected. A few studies deal with the plastic deformation mechanisms of AZ31 (Al 3%, Zn 1%). Some of the proposed models are summarized below:

Bussiba *et al*. [5] performed tensile tests at different strain rates on AZ31 at 177°C. The elongations they ob-

tained varied from 90% to 120%. They referred to grain boundary sliding [GBS] as a prevailing deformation mechanism.

Ben Hamo *et al*. [6] studied the microstructural changes of AZ31 after severe plastic deformation by Equal Channel Angular Extrusion (ECAE) at 350°C by means of optical microscopy, Scanning Electron Microscopy (SEM) and Transmission Electron Microscopy (TEM). They pointed to an increase in dislocation density and the occurrence of dynamic recrystallization. Jin *et al*. [7] studied ECAE of AZ31 at 225°C and noticed continuous dynamic recovery and recrystallization during ECAE. Dislocations were reported to form dislocation boundaries, which afterwards evolved to low- and high-angle grain boundaries.

Kim and Kim [8] conducted four stages of ECAE. The first and second stages were conducted at 320°C, while

the third and fourth stages were conducted at 250°C and 200°C, respectively. They reported grain refinement from 48 μm to 2.5 μm, as well as a bimodal grain size distribution after the first stage together with twinning and high dislocation densities after four stages of ECAE at 200°C - 320°C.

Tian et al. [9] performed creep tests of AZ31 at 200°C and proposed dislocation slip on basal and non-basal planes, together with twinning combined with dynamic recrystallization as the main deformation mechanisms. With respect to the active slip systems, they based their conclusion on contrast TEM investigation, namely, the $g \cdot b$ invisibility criterion.

Liu et al. [10] studied the deformation behavior of AZ31 during tension at the temperature range of 100°C - 250°C and at the strain rate range of 10^{-3} - 10^{-1} s^{-1}. They claimed that when the temperature was below the recrystallization temperature, twinning and dislocation slip—both basal and non-basal—were the dominant deformation mechanisms, while at temperatures above the recrystallization temperature, twinning-induced dynamic recrystallization (DRX) occurred as well.

Koike et al. [11] studied fatigue behavior at room temperature in tension cycles. They concluded that both twinning and prismatic slip contribute to the deformation.

Somekawa et al. [12] studied the creep properties of AZ31 at the temperature range of 200°C - 350°C. Calculation of stress exponent and activation energy led them to the conclusion that the major deformation mechanism is climb-controlled dislocation creep, which is controlled by pipe diffusion at low temperatures and by lattice diffusion at high temperatures.

Tan and Tan [13] focused on the occurrence of DRX in the case of AZ31B-O during tension tests at elevated temperatures, at the range of 200°C - 400°C. They witnessed grain refinement via deformation, mostly at 250°C. This grain refinement was attributed to dynamic continuous recrystallization, which involves progressive increase in grain boundary mis-orientation and conversion of low angle boundaries into high angle ones. Having conducted a TEM study, they reported on cells of tangled dislocation walls that are converted to a subgrain structure.

Watanabe et al. [14] referred to the high ductility of 196% exhibited by AZ31 during tension tests at 371°C. For their study they used coarse-grained (130 μm) commercial rolled AZ31 sheet. They pointed to glide control dislocation creep as the major deformation mechanism.

Mwembela et al. [15] conducted hot torsion tests in the temperature range of 180°C - 450°C. Having calculated the activation energy, they claimed that these values were consistent with the occurrence of rising dynamic recovery at 180°C - 300°C that in turn contributes to duc-

tility improvement. According to Mwembela et al. [15], dynamic recrystallization was initiated at about 300°C and 0.1 s^{-1} and became more widespread and characterized by larger grains as the temperature rose and the strain rate declined. They added that DRX was generally found near the grain boundaries, but nevertheless seemed sufficient to markedly improve ductility.

Myshlyaev et al. [16] conducted hot torsion tests from 180°C to 450°C and from 0.01 to 1.0 s^{-1} together with a TEM study. They reported on twins at 180°C with individual dislocations, with Dynamic Recovery (DRV) assumed to take place due to the existence of serrated grain boundaries. Deformation twins were detected at 240°C. as well together with higher dislocation density. Polygonal subgrains were observed at 300°C with walls of regularly arranged dislocations and random internal neworks. Equiaxed grains, smaller than the initial ones, were recorded at 360°C and higher. In addition to the deformation mechanisms briefly mentioned in the preceding paragraphs, it seems that most of the authors agree regarding the role of DRX at high temperatures. Assuming, however, that DRX is expected during FSW due to the high temperatures and the heavy plastic deformation, the current study focuses on the deformation process in a pre-recrystallized structure at relatively low temperatures.

2. Experimental

The material used in this study was a commercial AZ31B-H24 magnesium alloy, with a nominal chemical composition of Mg-3.0Al-1.0Zn (wt%) in the form of 3.175 mm thick 200 × 100 mm plates. The plates were butt welded using a CNC milling machine. An H-13 steel FSW tool was used, consisting of a pin 4.5 mm in diameter and 3 mm high, and a 20 mm diameter shoulder. The welding parameters were a rotational speed of $\omega =$ 2000 rpm and a transverse speed of $v = 20$ mm/min. All the welded specimens were radiographically checked prior to preparation of the creep specimen. Creep specimens were prepared with their longitudinal axis perpendicular to the seam, so that each specimen contained the welding nugget, the HAZ, the TMAZ and the parent material. Optical metallography was conducted with the aid of a Zeiss AZ10 optical microscope, while an FEI Inspect Scanning Electron Microscope (SEM) equipped with an INCA electron probe micro-analyser was used for SEM metallography. Creep tests both of parent AZ31-H24B material and of welded specimens were conducted at temperatures of 100°C, 200°C and 300°C and in the load range of 10 - 150 MPa. Specimens that underwent creep were used for a TEM study. TEM investigation involved using an FEI Titan 300 kV high-resolution TEM (HRTEM) and a Tecnai G^2 T20 200 kV TEM. The specimens for the TEM study were taken from

the neck of the broken creep specimen, tested at 100˚C and 50 MPa, as close as possible to the fracture surface. TEM study of the base material was carried out on an AZ31B-H24 non-welded specimen that had crept at 100˚C under 50MPa for 1215 hours up to an elongation of 5% without being broken, namely, an interrupted creep test specimen. A TEM approach simpler than the conventional $g \cdot b$ investigation was used in this study, as used by Regev *et al*. [17] for an AZ91D dislocation study. The samples were tilted into zone axes related to basal planes parallel to the incident electron beam, such as $\langle 11\bar{2}0 \rangle$. With these zone axes, dislocations on basal planes should appear straight and parallel, while their orientation (which is the orientation of the basal planes) can be obtained from the diffraction pattern. It should be emphasized that the active slip systems or the exact Burgers vector of the dislocations cannot be determined with this approach. Nevertheless, it provides evidence for the existence of non-basal dislocation segments.

3. Results

Optical micrographs of the various zones in the vicinity of the welding are given in **Figure 1**. The parent metal (**Figure 1(a)**) is characterized by a bi-modal grain size distribution, while grain coarsening is discernible in the Thermo-Mechanically Affected Zone (TMAZ), as can be seen in **Figure 1(b)**. The grain size of the Heat Affected Zone (HAZ) is relatively uniform (**Figure 1(c)**), though coarser than the fine grains of the parent metal. The grains of the nugget zone (**Figure 1(d)**) look deformed to some extent. Their size is uniform and finer compared with the parent material. Twinning can be observed in each zone, including the parent material. An SEM micrograph of the parent material under higher magnification is depicted in **Figure 2**. EDS analysis of ten bright particles, such as those indicated by arrows in **Figure 2**, showed that the particles contained a large amount of Mn, between 32.03 wt% and 54.45 wt%. No other phases were detected.
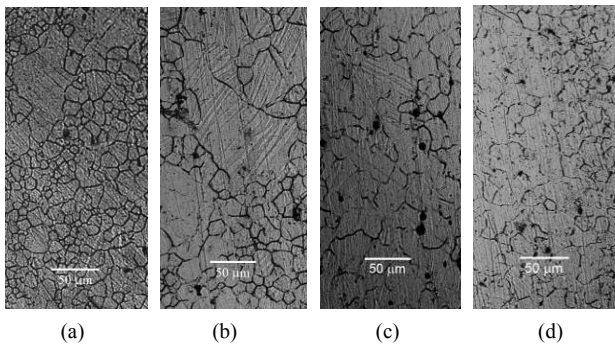
An optical micrograph of a broken creep specimen, which was taken from its neck next to the fracture line, is shown in **Figure 3**. This specimen had crept under 150 MPa at 100˚C, and the load had been applied horizontally. It can be seen that its grains are elongated and heavily twinned.

The elongations-to-fracture of non-welded AZ31 specimens varied between 24.6% and 53.7%, while the elongations-to-fracture of the welded specimens varied between 5% and 14%, with one exceptional specimen for which the recorded elongation was higher than 35%. As for the creep tests at 100˚C, the elongations-to-fracture varied from 24.6% to 41.9% in the case of the non-welded specimens, and from 5% to 10% for the welded specimens. According to the TEM procedure described in the previous section, basal (B) and non-basal (NB)
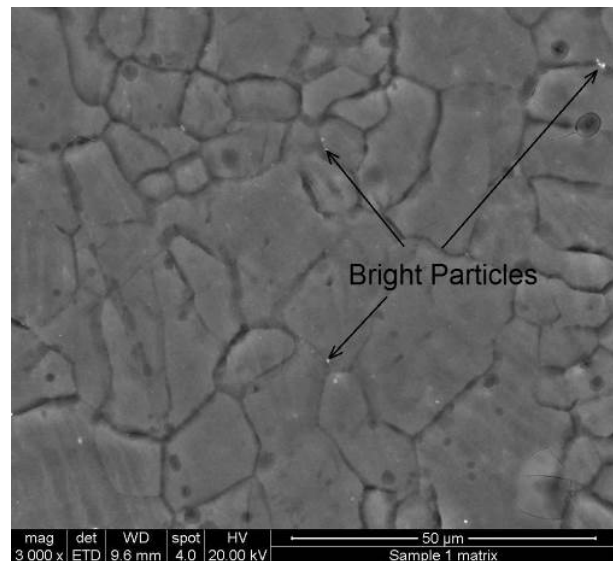

Figure 2. An SEM micrograph of the parent material.

Figure 1. Microstructure of the various zones: (a) parent material; (b) TMAZ; (c) HAZ; (d) nugget.
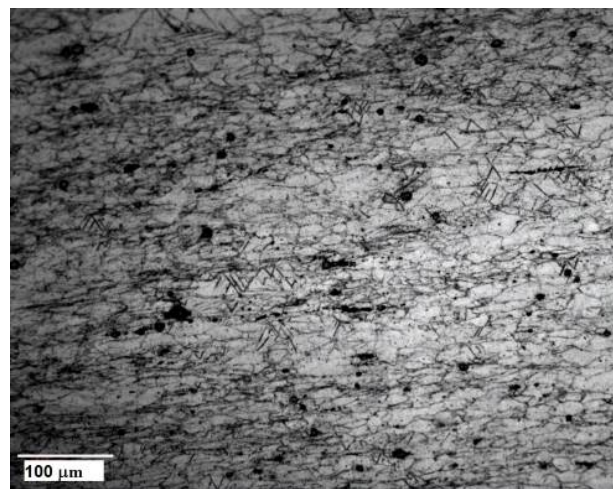

Figure 3. An optical micrograph of a broken creep specimen.

dislocation segments were observed in the welded specimen, as can be seen in **Figure 4**. Bright field (BF) TEM images taken from the welded crept specimen at $\langle 2\bar{1}10 \rangle$ are shown in **Figure 4**. A dislocation array can be seen in **Figure 4(a)**. This array lies partially on the basal plane. However, each of its dislocations contains non-basal segments. Non-basal dislocation segments together with basal segments are shown in **Figure 4(b)**, while **Figure 4(c)** shows the respective selected area diffraction pattern. In order to isolate the influence of the welding process, the same TEM procedure was repeated on a non-welded specimen that underwent creep for 1215 hours at 100°C under 50 MPa, as shown in **Figure 5**. It can be seen that most of the dislocation segments lie on the basal planes, both in the welded and in the non-welded specimens (**Figures 4** and **5** respectively).

For the sake of comparison, **Figure 6** was taken from the non-welded specimen that underwent creep for 1215 hours at 100°C under 50 MPa at $\langle 5\bar{1}43 \rangle$ zone axis in which the basal planes are inclined with respect to the incident electron beam and are therefore projected at the BF image. It can be clearly seen that the distribution of the dislocations is homogenous, namely, no planes are preferable for dislocation glide.

4. Discussion

Optical metallography shows that the bi-modal grain size microstructure of the parent material underwent extensive grain coarsening at the TMAZ. The grain size distribution of the TMAZ varies from a few microns to hundreds of microns, as can be seen in **Figure 1**. The HAZ, in contrast, is characterized by a relatively uniform grain size. The finer and relatively uniform grain size of the nugget can be attributed to DRX. The large differences in the average grain size probably influence the mechanical properties of each zone. Both this point and the existence of twinning at each zone, including the
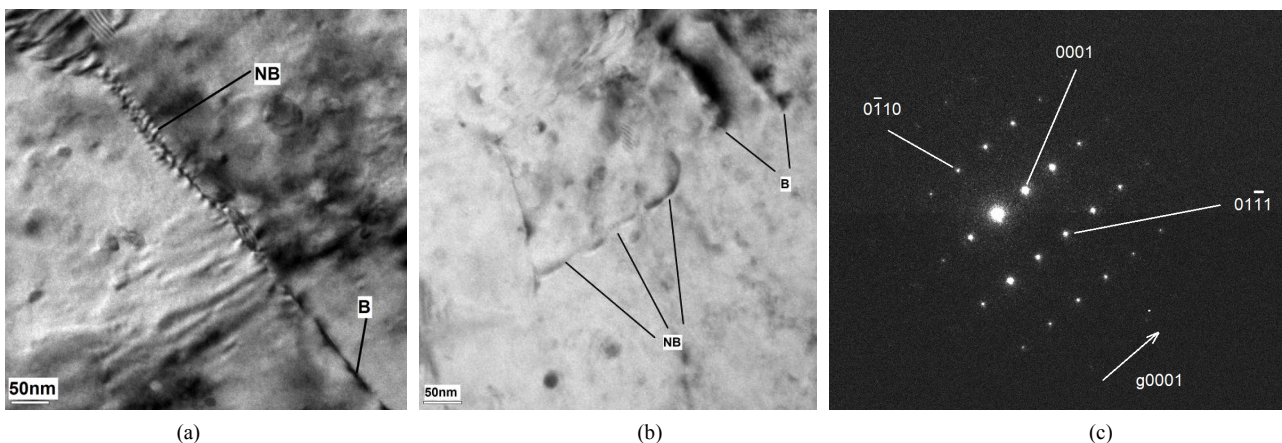

(a)   (b)   (c)

Figure 4. (a,b) Bright field TEM micrographs taken from a welded specimen at zone axis $\langle 2\bar{1}10 \rangle$ **(B-basal, NB-non- basal) (c) Electron diffraction pattern of zone axis** $\langle 2\bar{1}10 \rangle$.
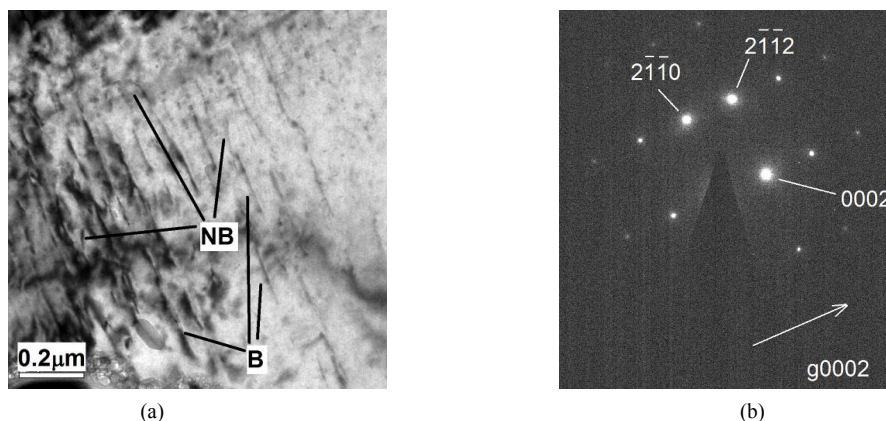

(a)   (b)

Figure 5. (a) Bright field TEM micrographs taken from a non-welded specimen at zone axis $\langle 01\bar{1}0 \rangle$ **(B-basal, NB-non-basal) (b) Electron diffraction pattern of zone axis** $\langle 01\bar{1}0 \rangle$.
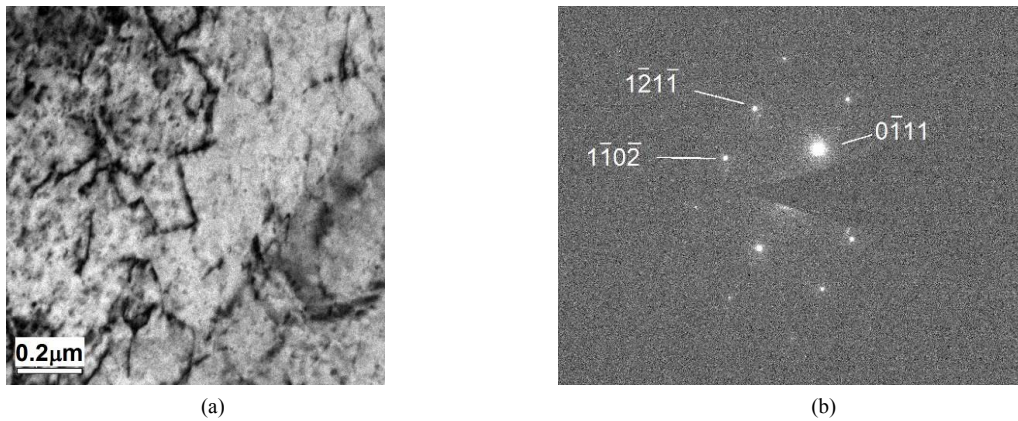

(a)

(b)

Figure 6. (a) Bright field TEM micrographs taken from a non-welded specimen at zone axis $\langle 5\overline{1}4\overline{3} \rangle$; (b) Electron diffraction pattern of zone axis $\langle 5\overline{1}4\overline{3} \rangle$.

parent material, will be discussed in the following paragraphs.

The expected phases according to the Mg-Al phase diagram [18] are Mg and β ($Mg_{17}Al_{12}$), and the chemical composition of the AZ31 alloy is within the two-phase region in which the Mg and β ($Mg_{17}Al_{12}$) phases coexist. The existence of these two phases was also reported in the literature by a number of researchers [5,9,15]. However, in this study no β phase was detected by EDS analysis. The only phase recorded besides the Mg matrix was the Mn-rich sub-micron particles. These results are in line with those reported by Ben Hamu *et al.* [6], who also did not detect a β phase and who identified the Mn-rich particles as Al_8Mn_5. It should be mentioned that the current study did not focus on phase characterization, and therefore X-ray Diffraction (XRD) was not performed. A possible explanation for the inability to detect the β phase is the low content of Al and hence of the β phase. Before referring to the operating plastic deformation mechanisms, the stability of the microstructure during creep should be examined. Unstable microstructure may lead to different creep behavior. This question was studied in the past by Regev *et al.* [19], who found that in the case of AZ91D alloy, the precipitation process of secondary β ($Mg_{17}Al_{12}$) occurring during creep influences the creep properties. The mechanism of this secondary β phase precipitation has been explained in detail elsewhere [20], and the reader is referred to this publication for a comprehensive discussion. It will only be mentioned here that secondary precipitation requires the formation of eutectic (supersaturated solid solution), while in the case of AZ31, according to its phase diagram [18] no eutectic structure is expected.

Figure 7 plots the minimum creep rate as a function of the applied stress for the base metal and the FSW samples tested at 100°C, 200°C and 300°C. The welded
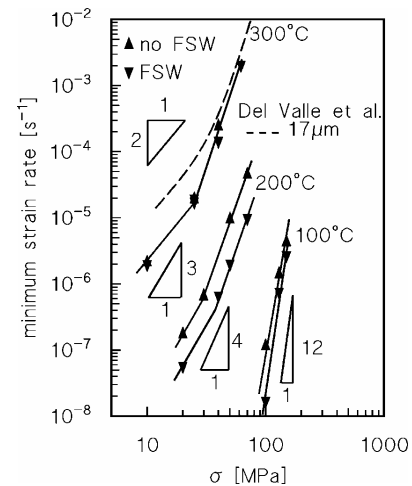

Figure 7. Minimum creep rate for base metal and FSW samples; the figure also shows the trend obtained by testing an AZ31 by using the changing strain rate technique [21, 22].

samples, quite unexpectedly, exhibited a lower creep rate when tested at 100°C and 200°C, although they ruptured after shorter durations. The minimum creep rate of the FSW samples tested at 300°C, in contrast, was for the most part equivalent to that of the base metal. In both cases, the dependence of the minimum creep rate $\left(\dot{\varepsilon}_m \right)$ on applied stress (σ) and temperature (T) can be tentatively described by a power law, in the form of:

$$\dot{\varepsilon}_m = A\sigma^n \exp\left(-Q/RT \right)$$

where n is the stress exponent, Q is the activation energy for creep, and A is a constant. Two different regimes seem to exist:

a) a high stress regime, characterized by high and temperature-dependent stress exponents (n = 4 - 12); the activation energy is close to the activation energy for

self-diffusion, 135 kJ/mol [1];

b) a low stress regime, where the stress exponent is lower (n = 2 - 3) and the activation energy is close to 100 kJ/mol.

The behaviour observed in the high stress regime is the typical response of materials tested above the power law breakdown, in which creep is controlled by climb. The case of the low-stress data is more difficult to interpret. A possible explanation of the low stress exponent is that in this region creep is controlled by viscous drag, *i.e.* dislocation glide is hindered by an atmosphere of Al solute atoms [2,22], as in Al-Mg alloys [1]. If this is the case, the stress exponent should be 3, and the activation energy should be equivalent to 142 kJ/mol (activation energy for diffusion of Al in Mg [2]), *i.e.* considerably higher than the experimental value, which is closer to the activation energy for grain boundary diffusion (92 kJ/mol). An alternative explanation, not considered in [22], is that at high temperatures and under low stresses GBS becomes the dominant mechanism. For comparison purposes, **Figure 7** also shows the trend observed by Del Valle and colleagues [23,24] while testing an AZ31 at 300˚C by the strain rate changes technique. These authors observed a well-defined low stress region, where n = 2 and Q was close to 92 kJ/mol. This low value of the stress exponent was not observed when the same material was tested under constant strain rate until fracture, since in that case n = 3 and the data substantially overlapped those obtained in the present investigation. This difference was attributed to grain growth, which resulted in a progressive increase in grain size during constant strain rate experiments. Grain growth can indeed be predicted to be more pronounced with increasing testing time, *i.e.* as strain rate decreases [23,24]. The same mechanism should also be operative in the material investigated in the present study, which was tested under constant load creep. It is thus reasonable to suppose that GBS can also play an important role in low-stress creep experiments.

In the case of the non-welded AZ31B specimens of the current study, the large elongations-to-fracture obtained at 100˚C, which can be referred to as the high stress regime, raise questions about the validity of the plastic deformation model of pure Mg. Namely, deformation occurs on the basal slip systems at room temperature, while at temperatures higher than 225˚C, prismatic and pyramidal systems become active as well [1-3]. As reported in the literature and summarized in the introduction to this paper, a number of deformation mechanisms were proposed by different researchers—GBS, twinning, DRX, dislocation slip on basal and non-basal planes [5-16].

Figures 5 and **6** seem to indicate that dislocation activity takes place on non-basal planes as well as on basal planes. However, in **Figure 5** the dislocations tend to concentrate on the basal planes, while in **Figure 6**, in which the basal planes are projected on the micrograph, the distribution of the dislocations is homogenous. Contrary to AZ91D, in which secondary β precipitation seems to block dislocation glide on the basal planes and hence to expedite cross-slip to non-basal planes [19], such a process is not expected in the case of AZ31B due to the stability of the microstructure. In any case, though basal planes are preferable for dislocation glide, it is quite obvious that dislocation glide takes place on other planes as well.

Twinning was observed in the current study, as can be seen from **Figures 1** and **2**. Yet it is well known that the amount of gross deformation that can be produced by twinning is relatively small, no more than a few percentage points, so twinning cannot explain the values of elongation obtained in the current study, at least not as a sole deformation mechanism. Nevertheless, when twinning exists it can contribute not by producing strain but rather by placing new slip systems at a favorable orientation with respect to the stress axis so that additional slip can take place.

Grain refinement indicates that DRX occurred during the welding process both at the nugget zone and to some extent at the adjacent zones. Yet in the literature DRX is reported to play a role as a deformation mechanism at temperatures higher than 100˚C. It seems that DRX is unlikely to be the major creep mechanism, though it still contributes to enhancing GBS by grain refinement and by placing new slip systems at a favorable orientation with respect to the stress axis as well as twinning.

Another important result is the place at which the fracture occurred, always at the TMAZ-HAZ interface of the advancing side, *i.e.*, the side at which the two velocity vectors (the rotation and the horizontal velocity) operate in the same direction. During FSW, material is transferred from the advancing side to the retreating side, on which the two velocity vectors are opposite. This material transfer may be responsible for the initiation of micro-cracks during creep, which eventually lead to fracture. Keeping in mind that the deformation mechanisms mentioned above are not influenced by grain size, and that the fracture appeared, at least in the specimens studied, at the TMAZ that had undergone grain coarsening, one may assume that the small elongations-to-fracture, measured in the case of the welded specimens, imply grain boundary sliding during creep. The extent to which the grains are elongated at the neck may point to the contribution of GBS. The increased amount of twinning found next to the fracture compared to the rest of the specimen leads to the conclusion that twinning takes place during creep as well as during welding.

In summary, the proposed mechanism is dislocation glide on basal and non-basal planes assisted by twinning

and GBS. Dislocation activity on non-basal planes can explain part of the large elongation-to-fracture due to additional active slip systems. Twinning contributes by placing new slip systems at a favorable orientation with respect to the stress axis, while GBS serves as an accommodation mechanism. The observed grain coarsening in the case of the welded specimens retards GBS, and therefore smaller elongations-to-fracture were recorded.

5. Conclusions

- Creep tests were carried out on friction stir-welded AZ31B-H24 specimens at 100˚C, 200˚C and 300˚C under 10 - 150 MPa.
- Optical metallography of the different zones in the welded specimens revealed a bi-modal grain size distribution at the parent metal, grain coarsening at the TMAZ, and a relatively uniform grain size at the HAZ. While the grains of the nugget zone look deformed to some extent, their size is uniform and finer than that of the parent material. Twinning can be observed at each zone, including the parent material.
- Two different creep regimes seem to exist: a high-stress regime in which creep is controlled by dislocation climb, and a low-stress regime in which GBS becomes the dominant mechanism.
- The elongations-to-fracture of the welded AZ31B-H24 specimens were markedly smaller than those of the non-welded ones. In the case of the welded specimen, the fracture always occurred at the TMAZ-HAZ interface of the advancing side.
- A dislocation study carried out by means of TEM showed evidence for non-basal dislocation slip. However, it seems that most dislocation glide occurs on the basal planes

6. Acknowledgements

REFERENCES

[1] S. S. Vagarali and T. G. Langdon, "Deformation Mechanisms in h.c.p. Metals at Elevated Temperatures I. Creep Behavior of Magnesium," *Acta Metallurgica*, Vol. 29, No. 12, 1981, pp. 1969-1981. doi:10.1016/0001-6160(81)90034-1

[2] S. S. Vagarali and T. G. Langdon, "Deformation Mechanisms in h.c.p. Metals at Elevated Temperatures II. Creep Behavior of a Mg-0.8% Al Solid Solution Alloy," *Acta Metallurgica*, Vol. 30, No. 6, 1982, pp. 1157-1170. doi:10.1016/0001-6160(82)90009-8

[3] K. Milička, J. Čadek and P. Ryš, "High Temperature Creep Mechanisms in Magnesium," *Acta Metallurgica*, Vol. 18, No. 10, 1970, pp. 1071-1082. doi:10.1016/0001-6160(70)90005-2

[4] J. R. Davis and P. Allen, "ASM Handbook," 10th Edition, ASM International, Ohio, 1990.

[5] A. Bussiba, A. Ben Artzy, A. Shtechman, S. Ifergan and M. Kupiec, "Grain Refinement of AZ31 and ZK60 Mg Alloys—Towards Superplasticity Studies," *Materials Science and Engineering A*, Vol. 302, No. 1, 2001, pp. 56-62. doi:10.1016/S0921-5093(00)01354-X

[6] G. Ben Hamu, D. Eliezer and L. Wagner, "The Relation between Severe Plastic Deformation Microstructure and Corrosion Behavior of AZ31 Magnesium Alloy," *Journal of Alloys and Compounds*, Vol. 468, No. 1-2, 2009, pp. 222-229. doi:10.1016/j.jallcom.2008.01.084

[7] L. Jin, D. Lin, D. Mao, X. Zeng, B. Chen and W. Ding, "Microstructure Evolution of AZ31 Mg Alloy during Equal Channel Angular Extrusion," *Materials Science and Engineering A*, Vol. 423, No. 1-2, 2006, pp. 247-252. doi:10.1016/j.msea.2006.02.045

[8] H. K. Kim and W. J. Kim, "Microstructural Instability and Strength of an AZ31 Mg Alloy After Severe Plastic Deformation," *Materials Science and Engineering A*, Vol. 385, No. 1-2, 2004, pp. 300-308.

[9] S. Tian, L. Wang, K. Y. Sohn, K. H. Kim, Y. Xu and Z. Hu, "Microstructure Evolution and Deformation Features of AZ31 Mg-Alloy During Creep," *Materials Science and Engineering A*, Vol. 415, No. 1-2, 2006, pp. 309-316. doi:10.1016/j.msea.2005.10.015

[10] J. Liu, D. Chen, Z. Chen and H. Yan, "Deformation Behavior of AZ31 Magnesium Alloy during Tension at Moderate Temperatures," *Journal of Materials Engineering and Performance*, Vol. 18, No. 7, 2009, pp. 966-972. doi:10.1007/s11665-008-9315-4

[11] J. Koike, N. Fujiyama, D. Ando and Y. Sutou, "Roles of Deformation Twinning and Dislocation Slip in the Fatigue Failure Mechanism of AZ31 Mg Alloys," *Scripta Materialia*, Vol. 63, No. 7, 2010, pp. 747-750. doi:10.1016/j.scriptamat.2010.03.021

[12] H. Somekawa, K. Hirai, H. Watanabe, Y. Takigawa and K. Higashi, "Dislocation Creep Behavior in Mg-Al-Zn Alloys," *Materials Science and Engineering A*, Vol. 407, No. 1-2, 2005, pp. 53-61. doi:10.1016/j.msea.2005.06.059

[13] J. C. Tan and M. J. Tan, "Dynamic Continuous Recrystallization Characteristics in Two Stage Deformation of Mg-3Al-1Zn Alloy Sheet," *Materials Science and Engineering A*, Vol. 339, No. 1-2, 2003, pp. 124-132. doi:10.1016/S0921-5093(02)00096-5

[14] H. Watanabe, H. Tsutsui, T. Mukai, M. Kohzu, S. Tanabe and K. Higashi, "Deformation Mechanism in a Coarse-Grained Mg-Al-Zn Alloy at Elevated Temperatures," *International Journal of Plasticity*, Vol. 17, No. 3, 2001, pp. 387-397. doi:10.1016/S0749-6419(00)00042-5

[15] A. Mwembela, E. B. Konopleva and H. J. McQueen, "Microstructural Development in Mg Alloy AZ31 during

Hot Working," *Scripta Materialia*, Vol. 37, No. 11, 1997, pp. 1789-1795. doi:10.1016/S1359-6462(97)00344-8

[16] M. M. Myshlyaev, H. J. McQueen, A. Mwembela and E. Konopleva, "Twinning, Dynamic Recovery and Recrystallization in Hot Worked Mg-Al-Zn Alloy," *Materials Science and Engineering A*, Vol. 337, No. 1-2, 2002, pp. 121-133. doi:10.1016/S0921-5093(02)00007-2

[17] M. Regev, E. Aghion, M. Bamberger, S. Berger and A. Rosen, "Dislocation Analysis of Crept AZ91D Ingot Castings," *Materials Science and Engineering A*, Vol. 257, No. 2, 1998, pp. 349-352.

[18] T. D. Massalski, "Binary Alloy Phase Diagrams," 2nd Edition, ASM, Ohio, 1987.

[19] M. Regev, A. Rosen and M. Bamberger, "Qualitative Model for Creep of AZ91D Magnesium Alloy," *Metallurgical and Materials Transactions A*, Vol. 32, No. 6, 2001, pp. 1335-1345. doi:10.1007/s11661-001-0224-5

[20] M. Regev, H. Rosenson and Z. Koren, "Microstructure Study of Particle Reinforced AZ91D and AM50 Magnesium Alloy," *Materials Science and Technology*, Vol. 23, No. 12, 2007, pp. 1485-1491. doi:10.1179/174328407X226554

[21] H. Sato and H. Oikawa, "Transition of Creep Characteristics of HCP Mg-Al Solid Solutions at 600-650K," In: D. G. Brandon, R. Chaim and A. Rosen, Eds., *Strength of Metals and Alloys*, Freund, London, 1991, pp. 463-470.

[22] S. Spigarelli, M. Regev, M. El Mehtedi, G. Quercetti and M. Cabibbo, "Analysis of the Effect of Friction Stir Welding on the Minimum Creep Rate of an Mg-3% Al-1% Zn Alloy," *Scripta Materialia*, Vol. 65, No. 7, 2011, pp. 626-629. doi:10.1016/j.scriptamat.2011.06.042

[23] J. A. del Valle, F. Penalba and O. A. Ruano, "Optimization of the Microstructure for Improving Superplastic Forming in Magnesium Alloys," *Materials Science and Engineering A*, Vol. 467, No. 1, 2007, pp. 165-171. doi:10.1016/j.msea.2007.02.088

[24] J. A. del Vall, M. T. Perez-Prado and O. A. Ruano, "Deformation Mechanisms Responsible for the High Ductility in a Mg AZ31 Alloy Analyzed by Electron Backscattered Diffraction," *Metallurgical and Materials Transactions A*, Vol. 36, No. 6, 2005, pp. 1427-1438. doi:10.1007/s11661-005-0235-8